BRITTLE FRACTURE NUCLEATION IN SA 533B-1 STEEL

A.Martín Meizoso, J.M.Rodríguez Ibabe, J.L.Viviente Solé and J.Gil Sevillano*

Cleavage origins ahead of previous crack fronts have been identified and the cleavage nucleation distance measured on brittle fracture surfaces of CT specimens of A 533B-1 steel whose critical cleavage stress and plastic properties were also measured. Using these data, the RKR model allows to predict a toughness- temperature relationship in good agreement with experimental values. The critical nucleation distance,the cleavage stress and other secondary evidence point to the bainitic packet size as being the most probable structural parameter controlling brittle fracture. An active non-critical role of the carbides in the fracture process is however not excluded.

INTRODUCTION

The Ritchie, Knott and Rice (1) "RKR" model for cleavage crack propagation provides with a rationale for linking the toughness with local, microscopic events taking place at the crack front under load. Successfully applied to explain the temperature and strain rate dependence of the brittle toughness of different materials (2-8), it has acquired widespread acceptance. The critical stress intensity factor, K_{Ic}, can be derived from the plastic properties of the material (temperature and strain rate dependent) and from its critical cleavage stress,σ_f, and critical distance, x_c (structure dependent).

The critical cleavage stress can be related to the minimum size of the slip-induced microcrack nuclei, t_c

$$\sigma_f = \beta K^B_{Ia} / \sqrt{t_c} \qquad (1)$$

*CEIT, Centro de Estudios e Investigaciones Técnicas de Guipúzcoa, Apdo.1555, 20080 San Sebastián (Spain).

with $\beta = 1,25$ for round and $\beta = 0,798$ for elongated nuclei, and K_{Ia}^{B} a local crack-arrest stress intensity factor of the boundary between the nucleating structural element and the metal matrix, apparently temperature and strain rate independent (Hahn (6)).

The critical cleavage nucleation distance is, as a first approximation, the average near-neighbour distance between nuclei, related with their areal density, (Underwood (9)) as,

$$x_c = 0,5 \; / \; \sqrt{N_a} \qquad (2)$$

Neither the nuclei size is uniform nor their space distribution regular and σ_f and x_c are only statistically determined parameters, dependent on the volume sampled by the plastic deformation preceeding cleavage fracture in potentially ductile materials.

The nature of the critical nuclei in bainitic or martensitic lath substructures is a controversial matter: covariant packets of laths, carbides and non metallic inclusions have been proposed by different authors (Bowen and Knott (10)).

Locations of cleavage nuclei just ahead of a previous crack front propagated by brittle fracture are identifiable by the radial river pattern of their associated characteristic cleavage facets (Rosenfield, Shetty and Skidmore (11)). This offers the possibility of directly measure the critical nucleation distance, x_c. Besides, information about the nature of the nucleus can be gathered, e.g., if some identifiable structural element is repeatedly found associated with the cleavage origin, such as non metallic inclusions (10). Given x_c, the areal density of nuclei follows from eq.(2). With this value, the minimum nucleating size of each structural element candidate to control brittle toughness of the material can be obtained from the frequency distribution of sizes measured by metallography. For the actual critical structural element, this minimum nucleating size must be consistent with that derived from the fracture stress, σ_f, through eq.(1), making use of the pertinent K_{Ia}^{B} value.

EXPERIMENTAL

It has been measured the distance from the fatigue (-196ºC) or subsequent ductile (-112ºC and -40ºC) crack front of a large number of nearest cleavage origins and the size of their associated characteristic facets on brittle fracture surfaces of 25 mm thick CT specimens of

SA 533B-1 steel with a tempered bainitic structure and T-S orientation. Figure 1 shows an example of a possible succession of crack nucleation events. Location of the crack origins -either at facet boundaries or at the interiors- was also recorded. Similar observations were also made on fracture surfaces of T-S oriented impact Charpy specimens broken in the upper part of the ductile-brittle transition temperature range (15ºC), with ductile propagations alternating with brittle bursts, where the cleavage nucleation distance was measured from the cleavage origin to the nearest ductile front. The results are summarized in Table 1

TABLE 1 - Cleavage origins triggering the propagation of a previous crack front. Mean distance to macrocrack front and average and minimum size of associated facets.

Specimen	T(ºC)	No.nuclei	x_c(μm) 95% c.l.	t(μm)* 95% c.l.	t_{min}(μm)*	Location(%) facet boundary	inter.
CT	-196	60	28 ± 7	34 ± 3	12	78	22
CT	-112	26	39 ± 9	35 ± 6	17	96	4
CT	- 40	44	35 ± 5	37 ± 4	18	100	0
Charpy V	15	18	59 ± 12	-	28	78	22

(*) Effective diameter, $\sqrt{ab}$, with a>b the axis of elliptical sections of the projected images of the facets.

Only at liquid nitrogen temperature (-196ºC) was initiation entirely brittle from the fatigue crack. A stable, ductile growth of the crack front of 9 ± 3 and 700 ± 70 μm was observed at, respectively -112 and -40ºC before the unstable, cleavage propagation. Considering the case of brittle crack initiation from a stationary crack (-196ºC), according to eq.(2), the density of effective nuclei is,

$$N_a(x_c=28\,\mu m) = 319\ mm^{-2} \qquad (3)$$

This value is barely modified if an average x_c value including the two values for cleavage nucleation from propagating cracks is used to compute N_a. For some reason the nucleation distance measured in Charpy specimens is significantly higher than that observed in CT specimens.

A detailed picture of facet size -distance combinations of the cleavage origins identified in CT specimens

broken in liquid nitrogen is given in fig.2. A broad spectrum of both parameters is found and a weak correlation between them is evident.

The majority of microcrack origins (88%) were located at facet boundaries and were essentially featureless or their nature was not discernible. No crack origin was found associated with non-metallic inclusions (their volume fraction in the steel was $f_V=0,038\pm0,003\%$ with an average effective size $\sqrt{ab}=4,4\pm0,2$ μm).

The critical cleavage fracture stress of the steel, σ_f, was also measured by means of low temperature (-196º) four-point bending tests with V-notched specimens as described by Griffiths and Owen (12). The average value of nine tests spanning through four orders of magnitude in strain rate (4.10^{-5}-0,12 s^{-1}) is, with its 95% c.l. margins,

$$\sigma_f = 1966\pm73 \text{ MPa} \qquad (4)$$

This value, with a 20% increase (2359 MPa) to compensate for the lower volume of the plastic zones of cracked vs notched specimens (Hahn (6), Kotilainen (13)), when used in conjunction with the measured x_c value (28μm) allows to predict -through the RKR model- critical stress intensity factors, K_{Ic}, in good agreement with experimental values for unstable fracture, fig.3. The latter were obtained by valid K_{Ic} tests according to ASTM E399 for -196ºC and from valid J values according to ASTM E813 for higher temperatures. Tensile stresses in the plastic zone ahead of the crack were computed with a numerical appproximation to the FEM results of Tracey (14) (Schwalbe (15), Tracey (16)). In the transition region the blunting effect pertinent for stationary cracks -limiting the maximum value of tensile stress (Rice and Johnson (17), McMeeking (18))- has been ignored in account of the sharper tip radius of the advancing ductile crack. The conventional elastic limit and work hardening exponent, n, of the steel were measured in tension at a wide range of temperatures. The former was fitted to functions based on Peierls-stress controlled glide and on obstacle controlled glide for low and moderate temperatures (Frost and Ashby (19)).

The agreement of the experimental K_{Ic} values with those computed making use of the measured x_c and σ_f emphasizes their representativeness and justifies the search of their consistent physical interpretation in the framework of the brittle fracture process (see (6) for a review).

DISCUSSION

Non-metallic inclusions can be discarded as cleavage nuclei for T-S fractures of this steel. According to evidence, nuclei relate mainly to boundaries between cleavage facets. Correspondence of the latter with sections of the bainite packets has been repeatedly proposed (Naylor and Krahe (20), Brozzo et al. (21), Kotilainen (13)) and is here demonstrated by the close agreement of the distributions of size and shape of bainite packets in metallographic sections and of projections of fracture facets on fracture surfaces (fig.4). The distributions were obtained from digitized SEM pictures. Average values are given in Table 2.

TABLE 2 - Average values of planar sections of bainite packets and projected images of cleavage facets of A 533B-1 steel.

	Packets	Facets
Minor axis, b(μm)	$8,8\pm0,3$	$8,7\pm0,3$
Eccentricty, a/b	$2,9\pm0,25$	$2,6\pm0,3$
N_a (mm^{-2})	5325	4982

(95% I.C. levels)

Bainite packets are thus the units of cleavage fracture of bainitic ferrite, its boundaries -in fact, ferrite high-angle boundaries- inducing deviations of the crack path orientation. However,location of most cleavage origins on packet boundaries does not give any proof on the control of cleavage nucleation by the packets themselves, as the boundaries are also preferred location of the largest carbides present. To discriminate among those two candidates to cleavage nuclei, the consistency of their available sizes and areal densities with the measured critical cleavage stress and nucleation distance (eqs.(1) and (3)) must be tested.

The most accepted value for the local critical stress intensity factor, K^B_{Ia}, for ferrite-carbide boundaries is 2,5 $MPa\sqrt{m}$ (6). According to eq.1 with σ_f=2359 MPa and β=1,25, the virtual critical carbide size is 1,75 μm.The areal density of carbides is given in fig.5; in fact,the experimental points shown are upper-bound values, as no correction has been made for the thickness of the foil in TEM observations or for the attack depth in SEM measurements. The actual density of carbides of the virtual critical effective size is under that required to justify the observed x_c value. The requirement is not met even if the largest dimension of the carbides, a, is ta-

ken as effective size. The density of carbides with $a>1,75$ μm is about six times the observed density of nuclei (319 mm^{-2}), nevertheless that means an "eligibility" -probability that a potential nucleus actually breaks under the stress field of the main crack- higher than 10^{-1}, values quoted for this parameter ranging from 10^{-2} to 10^{-3} (Curry and Knott (22), Wallin, Saario and Torronen (7)).

On the other hand, for ferrite-ferrite high angle boundaries, $K_{Ia}^{B}=5$ MPa$\sqrt{m}$ (6). With $\sigma_f=2359$ MPa and $\beta=0,798$, the virtual critical packet size (minor axis,b) is 2,86 μm. The density of packets in a planar section is 5325 μm^{-2}; about 5000 mm^{-2} have a minor axis $b>2,86$ μm (fig. 4) and the actual density of nuclei is only 319 mm^{-2},giving an eligibility of 6.10^{-2}. It can thus be concluded that bainite packet size most probably controls brittle fracture nucleation in the SA 533B-1 steel studied.

Some secondary evidence gives more support to this conclusion. Firstly, metallographic sections near fracture surfaces show microcracks stopped by packet boundaries, in agreement with other observations reported previously ((13),(21)). Secondly, the strain dependence of σ_f of bainitic steels can be explained by the strain induced size change of the nuclei -in contrast with mild steels- and this is only compatible with the packets being the critical nuclei, and never with the carbides of limited plasticity (Gil Sevillano (23)).

An active non-critical role of the carbides in the cleavage nucleation of this steel is nevertheless non excluded. Several observations -preferred location of cleavage origins at packet boundaries, presence of cracked packets in broken tensile specimens only close to cleavage fracture surfaces despite the general high level of plastic strain- suggest that cracking of bainite packets -formation of crack embryos- is induced by carbide cracking, thus influencing the "eligibility" of the controlling nuclei.

CONCLUSIONS

1. The critical cleavage distance for brittle crack initiation in a bainitic SA 533B-1 steel has been quantitatively determined identifiying cleavage origins at fracture surfaces ahead of previous crack front.

2. The measured x_c value, macroscopic toughness and cleavage fracture stress of this steel are only consistent with the control of brittle fracture by the bainite packet size.

LIST OF SYMBOLS

a,b	respectively, major and minor axis of ellipse
β	shape factor
K_{Ia}^{B}	local crack-arrest intensity factor for a given boundary
N_a	areal density (number of items per unit area).
σ_f	critical cleavage fracture stress
t	size of cleavage nucleus
t_c	critical size of cleavage nucleus
x_c	critical distance for cleavage nucleation

ACKNOWLEDGMENTS

This work is part of a project in collaboration with IBERDUERO,S.A., sponsored by OCIDE (Oficina de Coordinación de Investigación y Desarrollo Electrotécnico). Revision of the text by J.C.Zubillaga is gratefully acknowledged.

REFERENCES

(1) Ritchie, R.O., Knott, J.F. and Rice, J.R., J.Mech. Phys.Solids, Vol.21, 1973, p.395.

(2) Parks, D.M., J.Eng.Mater.Technol., Vol.98, 1976, p.30.

(3) Ritchie, R.O., Server, W.L. and Wullaert, R.A., Metall. Trans.A, Vol. 10A, 1979, p.1557.

(4) Curry, D.A. and Knott, J.F., Met.Sci.,Vol.10, 1976, p.1.

(5) Pineau,A., "Advances in Fracture Research", Vol.2, 1981, p.553. D.François, ed.,Pergamon Press,Oxford.

(6) Hahn,G.T., Metall.Trans.A.,Vol.15A, 1984,p.947.

(7) Wallin,K.,Saario,T. and Törrönen,K.,Met.Sci.,Vol.18, 1984, p.13.

(8) Gil Sevillano,J.,Rodríguez Ibabe,J.M. and Martín Meizoso, A., 8th.Int.Wheelset Congress,session I,

paper 2, Madrid, 1985.

(9) Underwood,G.E., "Quantitative Stereology", Addison-Wesley, Reading, Mass., 1970.

(10) Bowen,P. and Knott,J.F.,Met.Sci.,Vol.18,1984,p.225.

(11) Rosenfield,A.R.,Shetty,D.K. and Skidmore,A.J.,Metall.Trans., Vol.14A, 1983, p.1934.

(12) Griffiths,J.R. and Owen,D.R.J.,J.Mech.Phys.Solids, Vol.19, 1971, p.419.

(13) Kotilainen,H., Ph.D. Thesis, Helsinski University of Technology, Finland, 1980.

(14) Tracey,D.M.,J.Eng.Mater.Technol.,Vol.98, 1976,p.146.

(15) Schwable, J.Eng.Mater.Technol., Vol.98, 1976,p.186.

(16) Tracey,D.M.,J.Eng.Mater.Technol.,Vol.98,1976,p.187.

(17) Rice,J.R. and Johnson,M.A.,"Inelastic Behaviour of Solids", M.F.Kanninen et al.,eds.,p.641, McGraw-Hill, New York, 1970.

(18) McMeeking,R.M.,J.Mech.Phys.Solids,Vol.25,1977,p.357.

(19) Frost,H.J.and Ashby,M.F.,"Deformation-Mechanism Maps", Pergamon Press, Oxford, 1982.

(20) Naylor, V.P. and Krahe,P.R., Metall.Trans.,Vol.6A, 1975, p.594.

(21) Brozzo,P.,Buzzinelli,G., Mascanzoni,A. and Mirabile, M.,Met.Sci.,Vol.11, 1977, p.123.

(22) Curry,D.A. and Knott,J.F.,Met.Sci.,Vol.13,1979, p.341.

(23) Gil Sevillano, J.,Acta Metall., 1986, to be published.

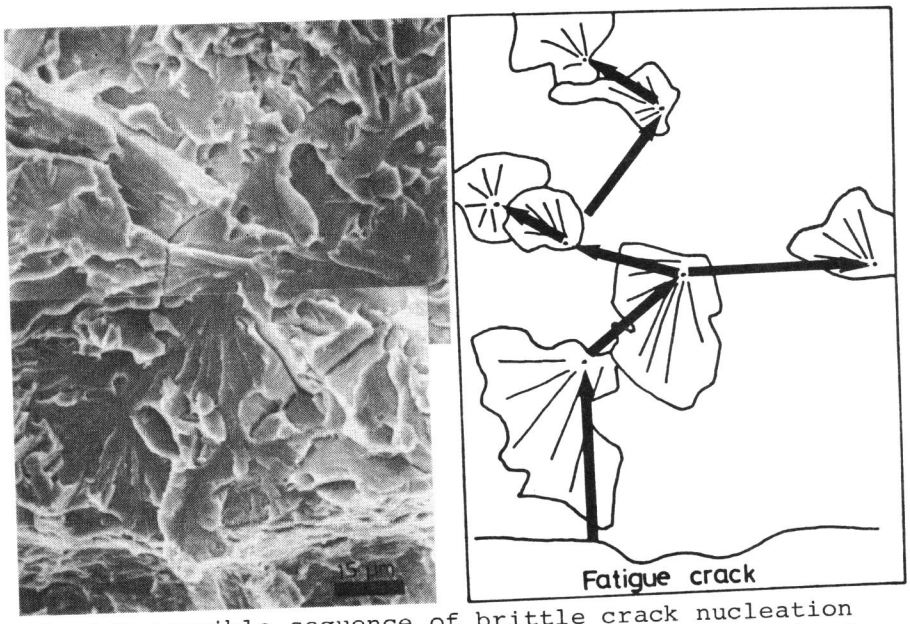

Fig.1 A possible sequence of brittle crack nucleation events after a very short stable ductile propagation from a fatigue crack (-112ºC).

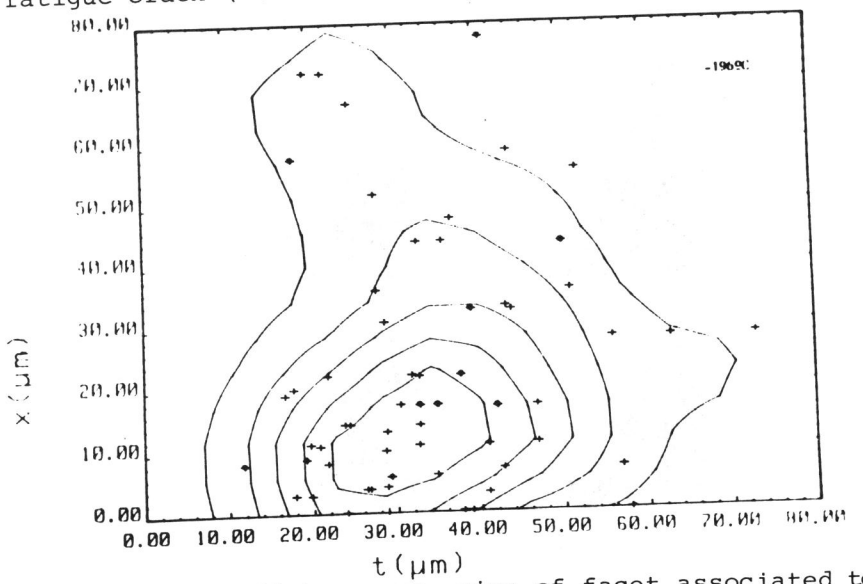

Fig.2 Nucleation distance vs. size of facet associated to cleavage origins. CT specimens,-196ºC. Different symbols pertain to different specimens.

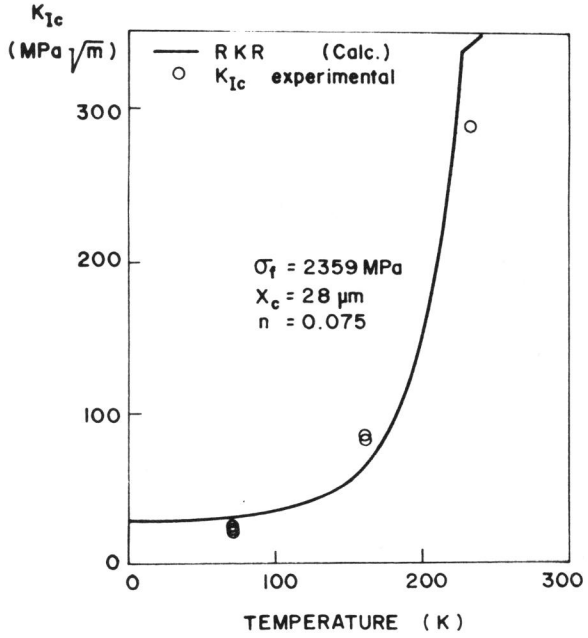

Fig.3 K_{Ic} vs.temperature.Predicted values according to the RKR model compared with experimental results.

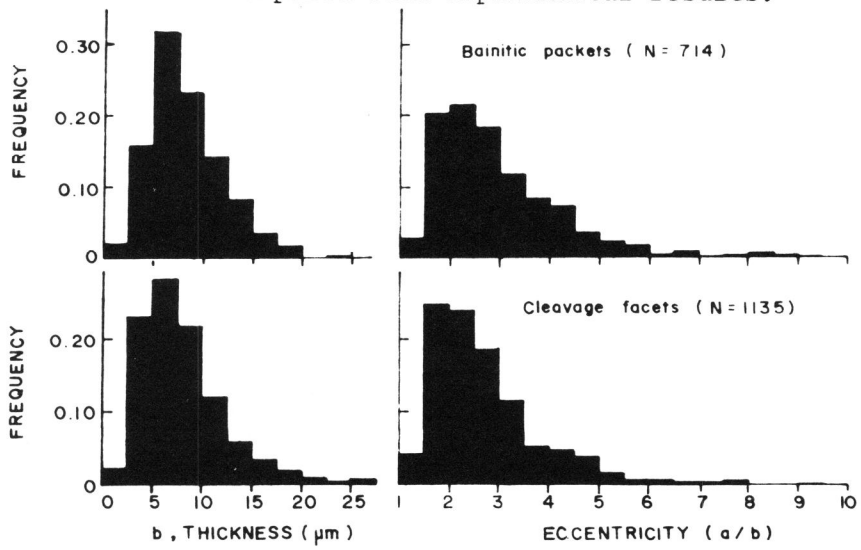

Fig.4 Distributions of thickness (minor axis of ellipse of equal area and maximum cord) and shape (eccentricity) of bainite packets and facets.

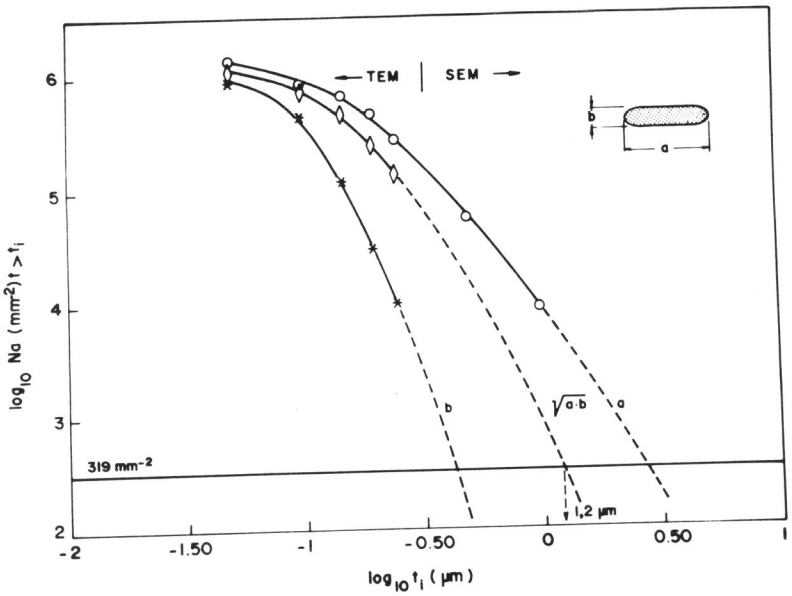

Fig.5 Double logarithmic plot of number of carbides of size $t > t_i$ per unit size vs. size t_i.